SUPPLEMENTAL MATERIAL

Ji Yoon Lee, Changwon Park, Yong Pil Cho, Eugine Lee, Hyongbum Kim, Pilhan Kim, Seok H. Yun, and Young-sup Yoon

Podoplanin-expressing Cells Derived from Bone Marrow Play a Crucial Role in Postnatal Lymphatic Neovascularization

Supplemental Methods

All protocols for animal experiments were approved by the Institutional Animal Care and Use Committees of Emory University.

Culture of BM-MNCs and SVEC4-10 cells

BM-MNCs were flushed from the tibias and femurs of 8-10 week old FVB mice or C57BL/6 eGFP transgenic mice (Jackson Laboratory), and fractionated by density gradient centrifugation with Histopaque®-1083 (Sigma, St. Louis, MO) to isolate mononuclear cells. Subsequently, the BM-MNCs were seeded at a density of 0.4-0.6 x $10^6/cm^2$ onto 100 mm culture dishes coated with rat plasma vitronectin (Sigma). To optimize culture conditions to generate LEPCs, four different combinations of media were employed (online-only Data Supplemental Table 1). During culture under these four conditions, non-adherent cells were discarded and only the attached cells were used for subsequent analysis and experiments. To differentiate MACS-sorted pod^+ or pod^- cells, and FACS-sorted pod^+CD11b^+ or pod^-CD11b^+ cells derived from cultured BM-MNCs into LECs, the cells were maintained in EBM-2 supplemented with 10% FBS, antibiotics, and cytokine cocktail (SingleQuots; Clonetics, Palo Alto, CA) for 7 days. The medium was changed on day 4 of the culture which was supplemented with the same cytokine cocktail. To maintain SVEC4-10 cells[1] (ATCC, CRL-2181), we used high glucose DMEM supplemented with 10% FBS and 4 mM L-glutamine adjusted to contain 1.5 g/L sodium bicarbonate.

Evaluation of plasticity of pod$^+$ cells in culture

Pod$^+$ cells isolated from 4 day-cultured BM-MNCs were cultured under the conditions supporting differentiation of each cell lineage. For endothelial cell differentiation[2], the pod$^+$ cells were plated onto vitronectin-coated dishes (1x 10^6 cells) and cultured in EGM-2 supplemented with 50 ng/ml VEGFA (R&D Systems, 293-VE-101) for 14 days. The resulting cells were stained with anti-vWF (Abcam) and anti-VE-cadherin (BD Biosciences) antibodies. For smooth muscle cell differentiation[3], we used high glucose DMEM/10% FBS with platelet-derived growth factor-BB (PDGF-BB, 10 ng/ml, Invitrogen, PHG0045). Antibodies against smooth muscle actin (Abcam, ab32575) and Desmin (Sigma, D1033) were used for immunocytochemistry. For fibroblast differentiation[4], the pod$^+$ cells were cultured in DMEM/10% FBS media, and were subjected to immunocytochemistry with anti-Vimentin (Santa Cruz, sc-7557) antibody. Secondary antibodies conjugated with Alexa 488 or Alexa 555 were used to visualize these primary antibodies.

Magnetic activated cell sorting (MACS) and fluorescence activated cell sorting (FACS)

For sorting of pod$^+$ cells with MACS, adherent cells 4 days after culture in the presence of VEGF-A, VEGF-C and EGF (all from R&D Systems, Minneapolis, MN) were trypsinized and resuspended in AutoMACS rinsing buffer. The cells were incubated with Syrian hamster anti-mouse pod antibody (Developmental Studies Hybridoma Bank, Seattle, WA) followed by biotin-conjugated goat anti-

hamster IgG antibody (Serotec, Brentwood, NH). After washing, the mixture was incubated with anti-biotin microbeads and subjected to MACS sorting (MiltenyiBiotec, Bergisch Gladbach, Germany). The same procedures were applied to sort pod^+ cells from SVEC4-10 cells. For sorting of pod^+ cells with FACS, the cultured cells or primarily isolated cells from BM of tumor bearing mice (refer to the mouse tumor model for the procedural details) were stained with FITC-conjugated Syrian hamster anti-mouse pod antibody (eBioscience, San Diego, CA) and were subjected to sorting with FACSVantageSE (Becton Dickinson, Franklin Lakes, NJ).

Quantitative RT-PCR

Total RNA and cDNA synthesis was performed as previously described[5]. Information on Taqman primer/probe sets (Biosearch Technologies, Novato, CA) used in this study is listed in online-only Data Supplemental Table 2. Relative mRNA expression of target genes was calculated with the comparative C_T method. All target genes were normalized to *Gapdh* in multiplexed reactions performed in triplicate. Differences in C_T values were calculated for each target mRNA by subtracting the mean value of *Gapdh* (relative expression = $2^{-\Delta CT}$).

Immunocytochemistry and immunohistochemistry

Immunocytochemistry and immunohistochemistry were conducted as previously described[6]. Cells were fixed with 100% methanol for 10 min at room temperature. After washing with PBS, the cells were blocked with 5% serum and subjected to

staining with primary antibodies, followed by incubation with secondary antibodies. DAPI was used for nuclear staining and the cells were visualized under a fluorescent microscope (Nikon, Melville, NY). For immunohistochemistry, samples frozen in OCT embedding medium (Sakura, Torrance, CA) were sectioned and stained with antibodies. Primary antibodies used were as follows: rabbit anti-mouse LYVE-1 (Millipore, Billerica, MA), rabbit anti-mouse PROX-1 (Millipore), rabbit anti-mouse VEGFR-3 (Santa Cruz Biotechnology Inc, CA), Syrian hamster anti-mouse pod (Developmental Studies Hybridoma Bank), rat anti-mouse CD45 (BD Biosciences). Cy2- or Cy3-conjugated goat anti-rabbit IgG (Jackson Immunoresearch Laboratories, West Grove, PA) and Cy3-conjugated goat anti-Syrian hamster IgG (Jackson Immunoresearch Laboratories) were used as secondary antibodies. The samples were examined with a Zeiss LSM 510 Meta confocal laser scanning microscope and LSM 510 Image software (CLSM, Carl Zeiss, Jena, Germany).

Flow cytometry

The FACS staining and analysis of mouse BM cells were performed as previously described[7]. Briefly, cells were resuspended with 100 μl of rinsing buffer and incubated with antibodies. After washing, the cells were analyzed with LSR II or FACScan (Becton Dickinson). As primary antibodies, we used PE-conjugated rat anti-mouse antibodies (Abs) against Sca-1, -FLK-1, -c-KIT, -CD45, or -CD11b (all from BD Biosciences), Alexa 488-conjugated hamster anti-mouse Ab against podoplanin (eBioscience), unconjugated rabbit anti-mouse Ab

against LYVE-1 (Acris, Herford, Germany) and biotin-conjugated rabbit anti-mouse Ab against VEGFR-3 (eBioscience). As a secondary Ab, biotinylated goat anti-rabbit IgG (Jackson Immunoresearch Laboratories) was used with APC-conjugated Streptavidin (eBioscience) to detect the biotinylated signals. Flow cytometric data were analyzed with FlowJo (Tree Star Inc., Ashland, OR) using appropriate controls with proper isotype-matched IgG and unstained controls.

LEC proliferation assay

The sorted pod$^+$ and pod$^-$ cells (2.5 x 10^3) from 4 day-cultured BM-MNCs were mixed with human dermal lymphatic endothelial cells (hDLECs, 1.5 x 10^4) (Cambrex), which were pre-labeled with cell tracker CM-DiI (Invitrogen), seeded onto 96 well culture plates and co-cultured in EGM media with 1% FBS. Twenty four hours later, cells were stained with Ki67 antibody (Abcam, 1:200) and counterstained with DAPI. Cells positive for DiI, Ki67 and DAPI were counted.

For statistical analysis, we counted 714 cells in the PBS control (7 fields x ~34 cells/field x 3 independent experiments), 798 cells in the pod$^+$ group (7 fields x ~38 cells/field x 3 independent experiments) and 756 cells in the pod$^-$ group (7 fields x ~36cells/field x 3 independent experiments).

Mouse Cornea Model

The mouse corneal assay was performed as previously described[8]. FVB mice (8-10 week old males) were anesthetized with an intraperitoneal injection of ketamine and xylazine. Subsequently, a micropocket was created using a

modified von Graefe knife followed by implantation of a micropellet (0.35 mm) of sucrose aluminum sulfate coated with 12% hydron (poly (2-hydroxyethyl methacrylate), Sigma) containing 250 ng of VEGF-C and 80 ng of FGF-2 into the pocket. The pellet was positioned 0.6-0.9 mm from the corneal limbus and 1 x 10^6 carbocyanine dye CM-DiI (DiI; 1.5 μg/ml; Invitrogen, Carlsbad, CA)-labeled 4-day cultured pod^+ cells were injected into the surrounding area in the cornea. Seven days after pellet implantation, eyeballs were isolated, fixed with 4% PFA, and sectioned for immunohistochemistry.

Skin and Ear Wound Models

After shaving hairs and aseptic preparation, full-thickness excisional skin wounds (one per mouse) were created on the backs or ears of the mice using 6-mm skin biopsy punches (Baker Cummins Dermatological, Livingston, NJ). Half a million pod^+ cells or pod^+ $CD11b^+$ cells labeled with DiI or derived from GFP mice in 100 μl PBS were then injected into the wound bed at four different sites around the wound. Seven days later, the wound tissues were harvested including a perimeter of 1 to 2 mm of normal skin tissue, fixed with 4% PFA, and sectioned for immunohistochemistry. To examine lymphangiogenic cytokine expression by qRT-PCR, 2 x 10^6 of pod^+ or pod^- cells from 4 day-cultured BM-MNCs in 100 μl PBS or the same volume of PBS were injected into wounded tissues of backs of diabetic C57BLKS/J-m $^{+/+}$ Leprdb (db/db, 8-10 week old) mice. Seven days later, the skin tissues were harvested and subjected to qRT-PCR.

Mouse Tumor (Melanoma) Model

First, to evaluate the in vivo contribution of pod^+ cells derived from cultured BM-MNCs to lymphatic vessel formation (Figure 3C), 2 x 10^6 tumor cells (B16-F1 melanoma cell line) in 100 µl PBS were subcutaneously injected into the middle dorsum of C57BL/6 mice. Seven days later, when the primary tumors had reached the size of 1 cm in diameter, Dil-labeled pod^+ cells isolated from cultured BM-MNCs were injected into the tumor vicinity and the mice were sacrificed 7 days later. Second, to analyze the presence of pod^+ cells in BM and peripheral blood (PB) and pod^+CD11b^+ cells in BM (Figure 5A, 5C, online-only Data Supplemental Figure S5 and S6), FACS analysis was performed on BM-MNCs or PB-MNCs obtained from mice which had received the tumor cells 7 days before. Third, to determine the lymphvasculogenic potential of freshly isolated pod^+ cells from tumor bearing mice (Figure 6A and 6B), B16-F1 melanoma cells were injected into the backs of C57BL/6 mice for tumor induction and 7 days later, pod^+ cells were isolated from BM-MNCs of these mice using FACS, labeled with Dil and injected into mouse wound models. Seven days later, the mice were sacrificed and subjected to immunohistochemistry as described above.

In vivo confocal microscopy

We used a custom-made laser scanning confocal microscopy system that is housed in Wellman Center for Photomedicine at Harvard Medical School, as previously described[9], to track pod^+ cells and monitor LECs in vivo in live mice. An ear wound model and a corneal micropocket model were created as

described above and 1 x 10^6 pod^+ cells labeled with DiI were injected into the wound bed. After 7 days, mice were anesthetized by an intraperitoneal injection of ketamine and xylazine and placed on the heated plate on the motorized stage. Cy5.5-conjugated mouse anti-LYVE-1 antibody was intradermally injected to stain LECs in vivo. Fluorescence signals of DiI and Cy5.5 were detected after excitation with a 532 nm continuous wave (CW) laser (Cobalt, Stockholm, Sweden) and a 635 nm CW laser (Coherent, Inc., Santa Clara, CA), respectively through a 579 ± 17 nm and a 692 ± 20 nm band pass filter (Semrock, Inc., Rochester, NY), respectively.

Measurement of lymphatic capillary density

After implantation of tumors (melanomas) and injection of pod^+ or pod^- cells or the same volume of PBS as described above, tumors and surrounding peritumoral tissues including skin were harvested and subjected to immunohistochemistry with a VEGFR-3 antibody for lymphatic vessel staining[6]. Lymphatic capillary density (number of $VEGFR\text{-}3^+$ lymphatic vessels) was calculated from at least 10 randomly selected fields.

Statistical Analysis

Statistical analyses were performed with the Mann-Whitney U test for comparisons between two groups and the Kruskal-Wallis ANOVA test for more than two groups. Hence, the statistical analysis for Figure 2A, 2B, 2C, Figure 5 and Online Supplemental Figure S6 was performed with the Mann-Whitney U

test and the analysis for Figure 4C, E and F with the Kruskal-Wallis ANOVA test. GraphPad Prism 4 (Graph-Pad Prism, GraphPad Software Inc, SanDiego) was used for the analyses. *P* values < 0.05 were considered to denote statistical significance.

Online supplemental material

Online-only Data Supplemental Figure 1 shows the expression level of LEC markers in pod^+ cells and SVEC4-10 cells. Online-only Data Supplemental Figure 2 shows plasticity of pod^+ cells from BM-MNCs. Online-only Data Supplemental Figure 3 shows incorporation of injected pod^+ cells in pod^+ lymphatic endothelium. Online-only Data Supplemental Figure 4 describes engraftment of pod^+ cells adjacent to lymphatic vessels. Online-only Data Supplemental Figure 5 shows expression of podoplanin in c-KIT^+ cells of BM-MNCs of tumor bearing mice. Online-only Data Supplemental Figure 6 shows that the frequency of pod^+cD11b^+ cells increases in BM of tumor bearing mice. Online-only Data Supplemental Figure 7 shows comparison of morphology between pod^+CD11b^+ cells and pod^-CD11b^+ cells. Online-only Data Supplemental Video 1 and 2 show the projection view of the confocal images of Figure 3C and 3E, respectively. Online-only Data Supplemental Table 1 shows the culture conditions for LEPCs. Online-only Data Supplemental Table 2 describes the mouse-specific primers and probes for qRT-PCR.

Supplemental Figures

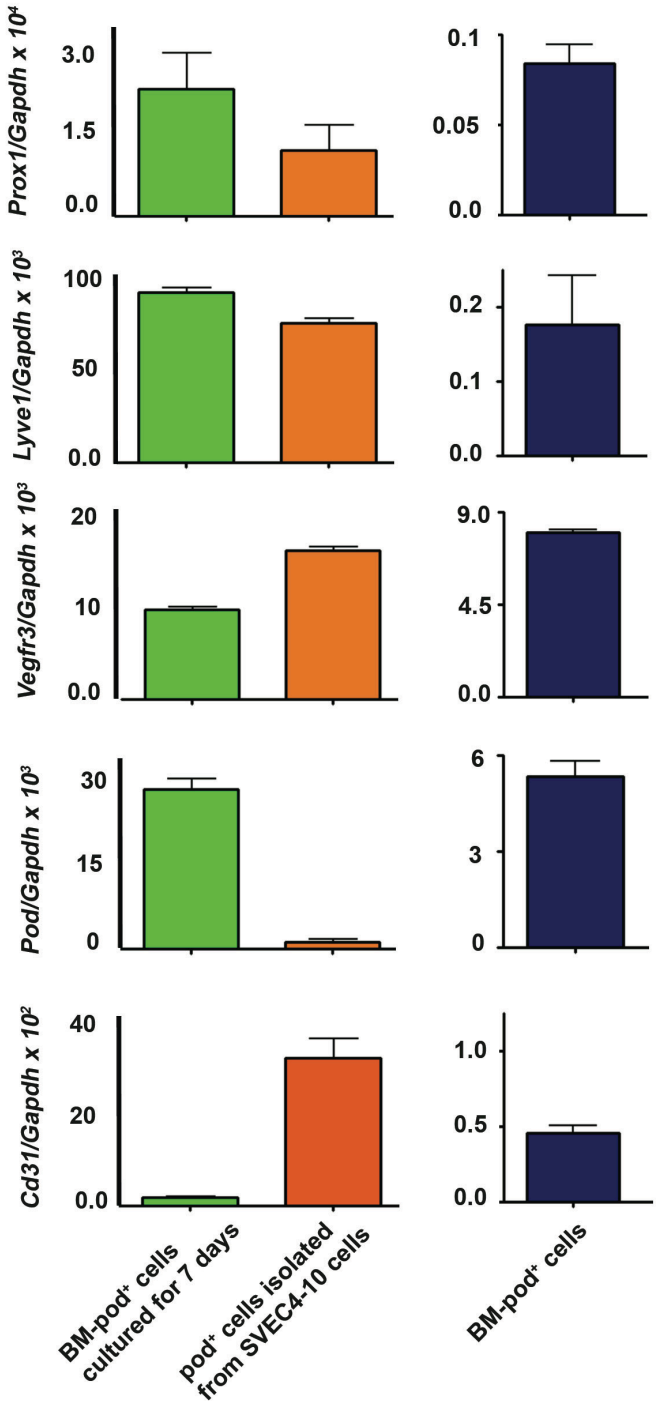

Supplemental Figure 1. The expression of LEC markers in pod$^+$ cells from BM-MNCs and SVEC4-10 cells. Pod$^+$ cells derived from BM-MNCs and SVEC4-10 cells were subjected to qRT-PCR analyses. BM-Pod$^+$: pod$^+$ cells MACS-isolated from 4 day-

cultured BM-MNCs, BM-pod$^+$ cells cultured for 7 days: pod$^+$ cells MACS-sorted from 4 day-cultured BM-MNCs and cultured for another 7 days. Graphs were presented as mean ± SE from three independent experiments.

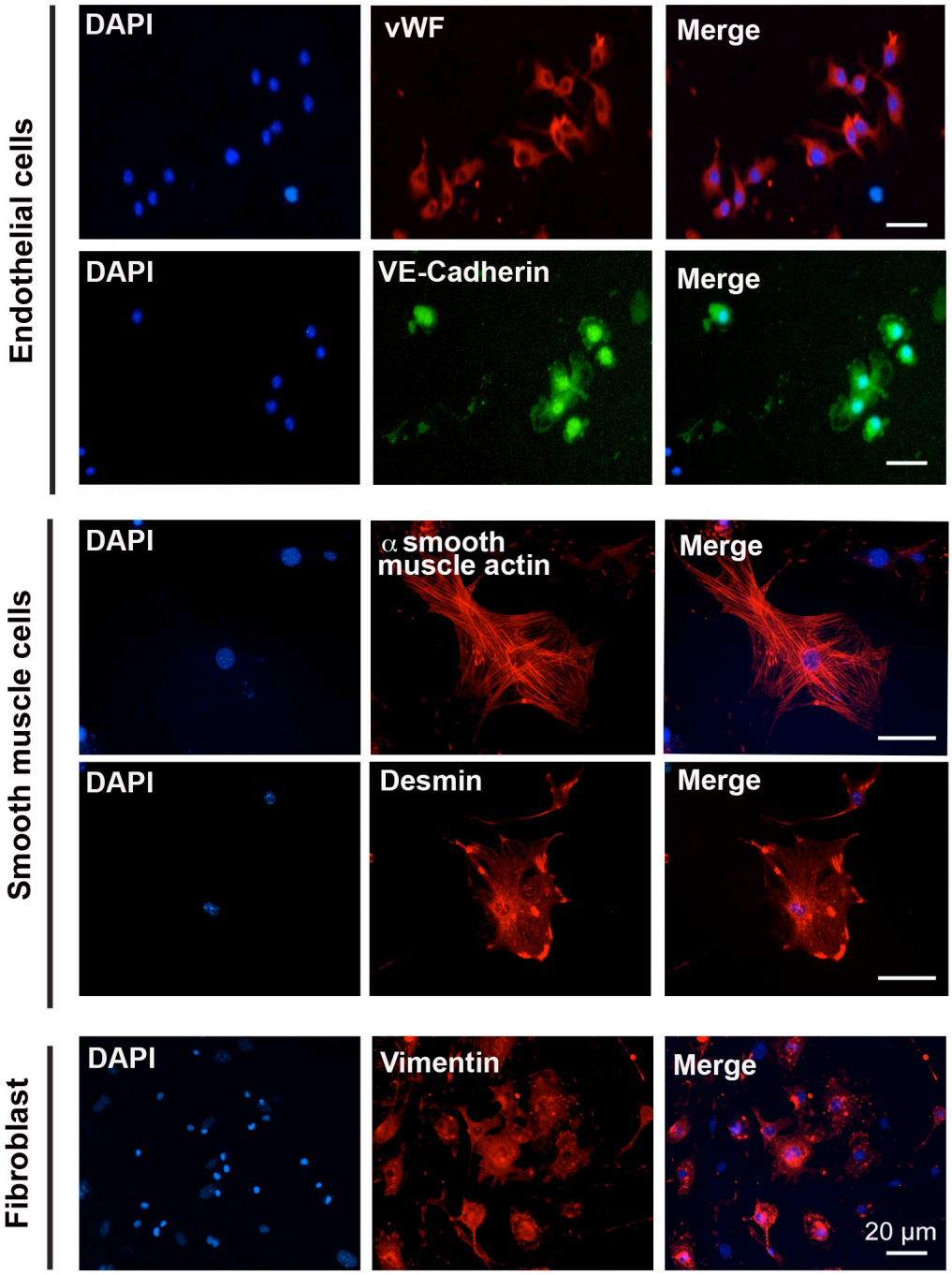

Supplemental Figure 2. BM-MNC-derived pod$^+$ cells can differentiate into endothelial cells, smooth muscle cells and fibroblasts. Pod$^+$ cells from 4 day-

cultured BM-MNCs were further cultured under the various differentiation conditions for indicated cell lineages. The resulting cells were immunostained with each lineage markers. Representative images from three independent experiments are shown. vWF; von Willebrand Factor. Scale bar = 20 um

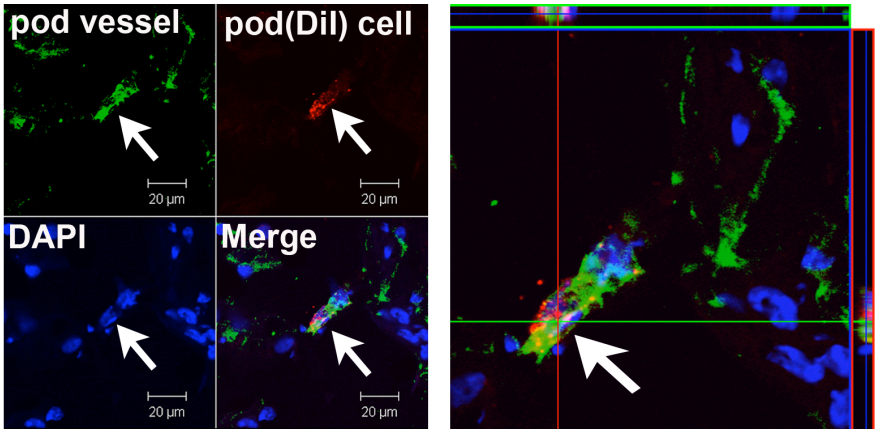

Supplemental Figure 3. Lymphvasculogenesis by the injected pod$^+$ cells in a mouse ear wound model. Mice that had received ear wound surgery were injected with DiI-labeled, pod$^+$ cells (red). Seven days later, ear tissues from the mice were harvested and sectioned for immunostaining for podoplanin (green, pod vessel). The arrow indicates incorporation of pod$^+$ cells within lymphatic vessels stained positive for podoplanin. DAPI (blue) for nuclei staining. Representative images from at least two independent experiments are shown. n=3 per experiment. Scale bar = 20 μm.

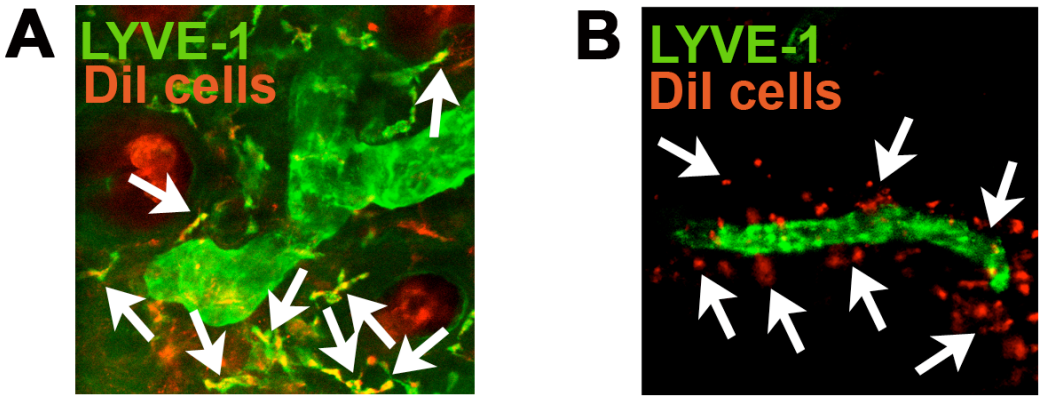

Supplemental Figure 4. Engraftment of pod$^+$ cells in lymphatic vessels. The sorted cells from the BM-MNCs were injected into mice. Seven days later, ear (A) and cornea tissues (B) from the mice were subjected to whole-mount immunostaining for podoplanin (red) and LYVE-1 (green). The arrows indicate engraftment of pod$^+$ cells adjacent to lymphatic vessels. Representative images from at least two independent experiments are shown. n=3 per experiment.

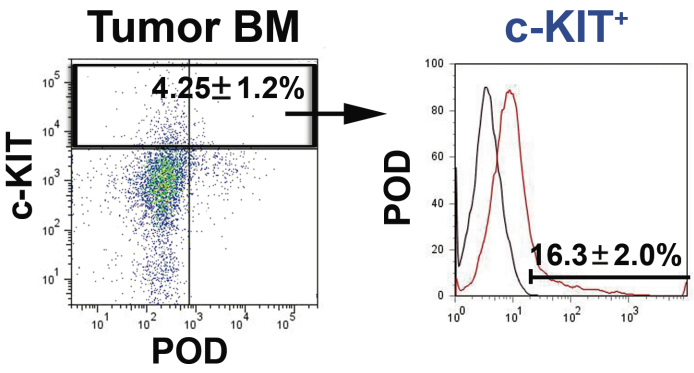

Supplemental Figure 5. Expression of Podoplanin in c-KIT$^+$ cells of BM-MNCs of tumor bearing mice. BM-MNCs of tumor (B16-F1 melanoma cells) bearing mice were subjected to FACS analysis for c-KIT and pod expression. Percentages were presented as mean ± SE from three independent experiments.

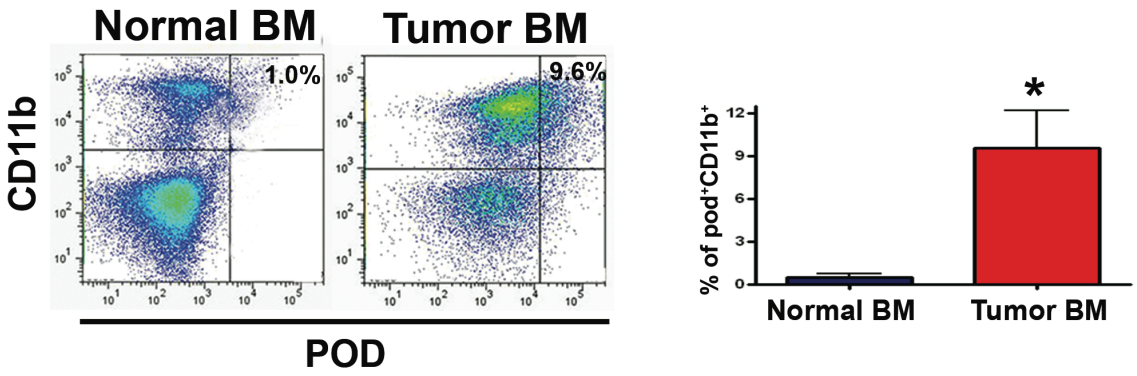

Supplemental Figure 6. The frequency of pod^{+}CD11b^{+} cells increases in BM of tumor bearing mice. BM-MNCs harvested from mice that had been injected with B16-F1 Melanoma cells were subjected to FACS analyses for pod and CD11b expression. Graphs were presented as mean ± SE from three independent experiments (n=3 per experiment, * $P < 0.05$)

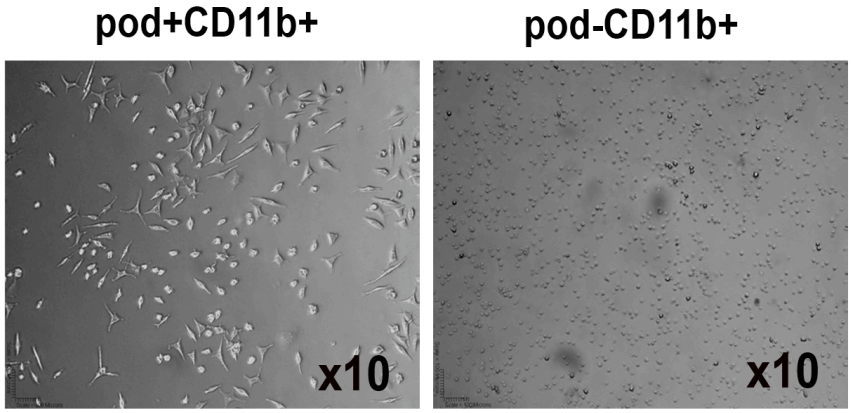

Supplemental Figure 7. Comparison of morphology between pod^{+}CD11b^{+} cells and pod^{-}CD11b^{+} cells. The sorted cells from the BM-MNCs were seeded on vitronectin-coated plates in EGM, cultured for 24 hours and monitored under an inverted microscope. The pod^{+}CD11b^{+} cells were attached as a monolayer and displayed round cobblestone- and spindle-shaped morphologies, whereas the pod^{-}CD11b^{+} cells were floating and maintained small round shape morphology. Magnification, x 10.

Supplemental Tables

Table S1. Culture conditions for LEPCs

	A	C	AC	ACE
5% FBS	+	+	+	+
VEGF-A (50 ng/ml)	+		+	+
VEGF-C (100 ng/ml)		+	+	+
EGF (10 ng/ml)				+
Ascorbic acid (100 ng/ml)	+	+	+	+

A, VEGF-A; C, VEGF-C; E, EGF; EGM, EBM-2 + SingleQuots

Table S2. Primers and probes for quantitative RT- PCR

Genes	Unigene	Primers and Probes (5`-3`)	
		Forward	CTTCCGCCATCCCTTTCC
		Reverse	CCGGAGGGAGCACCTAGTG
Prox1	NM008937	Probe	CTGCCCTTGATGGCTTATCCATTTCAGA
		Forward	CAGCAGCAGCGCCTACTTG
		Reverse	CCGGGTGGTGGCAGAA
Lyve1	NM053237	Probe	TCATCCCCTGACTCCACAACACC
		Forward	TGGCAAGGCACCTCTGGTA
		Reverse	TGAGGTGGACAGTTCCTCTAAGG
pod	NM010329	Probe	CAACGCAGAGAGAGCGTGGGACG
		Forward	TGCTGAAAGAGGGCGCTACT
		Reverse	TGCCGATGTGAATTAGGATCTTG
Vegfr3	NM008029	Probe	AGCACCGTGCCCTGATGTCGGA
		Forward	TCCCCGAAGCAGCACTCTT
		Reverse	ACCGCAATGAGCCCTTTCT
Cd31	NM001032378	Probe	CAGTCAGAGTCTTCCTTGCCCCATGG
		Forward	CATCTTCAAGCCGTCCTGTGT
		Reverse	CAGGGCTTCATCGTTACAGCA
Vegfa	NM0010252503	Probe	CCGCTGATGCGCTGTGCAGG
		Forward	CAGCAAGACGTTGTTTGAAATTACA
		Reverse	GTGATTGGCAAAACTGATTGTGA
Vegfc	NM0000745	Probe	CCTCTCTCACAAGGCCCCAAACCA
		Forward	GCAAATCGCGCACTCTGA
		Reverse	TGGCAAGACTTTTGAGCTTCAA
Vegfd	NM010216	Probe	ACTGGAAGCTGTGGCGATGCCG
		Forward	TGCTTCCGGAGCTGTGATCT
		Reverse	CGGGCTGCTTTTGTAGGCT
Igf1	NM0011112741	Probe	AGGAGACTGGAGATGTACTGTGCCCCAC
		Forward	GGGCTGTGTTCCCATCCAT
		Reverse	AGGAGTCCTTCTGACCCATACCT
Ang1	NM0096403	Probe	TGGGCCGACCCCGTCACC
		Forward	GTCACGGAAATACTCCAGTTGGT
		Reverse	CCGTTTTGGATCCGAGTTTATACT
bFgf	NM0080062	Probe	TGTGGCACTGAAACGAACTGGG
		Forward	CTGACCCAAACATCCGAGTTG
		Reverse	TTCCCATTGCCACGATAACAA
Hgf	NM0104274	Probe	TGCTCTCAGATTCCCAAGTGTGACGTGT
		Forward	TGGTGTGTGACGTTCCCATT
		Reverse	CAGCACGAGGCTTTTTTGTTG
Il1	NM0083613	Probe	ACAGCTGCACTACAGGCTCCGAGATGA

		Forward	CGTGTTCCTACCCCCAATGT
		Reverse	TGTCATCATACTTGGCAGGTTTCT
Gapdh	NM001001303	Probe	TCGTGGATCTGACGTGCCGCC

Supplemental Legends for The Videos

Legend for Video 1. Representative projection view of the engrafted podoplanin$^+$ cells in a tumor model.

Mice which had been implanted with tumor cells (B16-F1 Melanoma) were injected with DiI-labeled pod$^+$ cells (red) and the tissues were harvested 7 days later for immunohistochemistry. Representative confocal images from peritumoral subcutaneous tissues demonstrated that DiI-labeled pod$^+$ cells were incorporated into lymphatic vessels and exhibited a LEC marker, LYVE-1 (green).

Legend for Video 2. Representative projection view of the engrafted podoplanin$^+$ cells in a wound model.

A skin wound model was created and the pod$^+$ cells from GFP mice were injected into peri-wound tissues. Seven days later, the tissues were harvested and immunostained for LYVE-1 (red). Confocal microscopic examination with 3D reconstruction showed that injected pod$^+$ GFP cells (arrows) were incorporated into the lymphatic vessels and expressed LYVE-1 (red).

Supplemental References

1. Ledgerwood LG, Lal G, Zhang N, Garin A, Esses SJ, Ginhoux F, Merad M, Peche H, Lira SA, Ding Y, Yang Y, He X, Schuchman EH, Allende ML, Ochando JC, Bromberg JS. The sphingosine 1-phosphate receptor 1 causes tissue retention by inhibiting the entry of peripheral tissue T lymphocytes into afferent lymphatics. Nat Immunol. 2008;9:42-53.
2. Ferreira LS, Gerecht S, Shieh HF, Watson N, Rupnick MA, Dallabrida SM, Vunjak-Novakovic G, Langer R. Vascular progenitor cells isolated from human embryonic stem cells give rise to endothelial and smooth muscle like cells and form vascular networks in vivo. Circ Res. 2007;101:286-294.
3. Ross JJ, Hong Z, Willenbring B, Zeng L, Isenberg B, Lee EH, Reyes M, Keirstead SA, Weir EK, Tranquillo RT, Verfaillie CM. Cytokine-induced differentiation of multipotent adult progenitor cells into functional smooth muscle cells. J Clin Invest. 2006;116:3139-3149.
4. Moreau JE, Chen J, Bramono DS, Volloch V, Chernoff H, Vunjak-Novakovic G, Richmond JC, Kaplan DL, Altman GH. Growth factor induced fibroblast differentiation from human bone marrow stromal cells in vitro. J Orthop Res. 2005;23:164-174.
5. Cho HJ, Lee N, Lee JY, Choi YJ, Ii M, Wecker A, Jeong JO, Curry C, Qin G, Yoon YS. Role of host tissues for sustained humoral effects after endothelial progenitor cell transplantation into the ischemic heart. J Exp Med. 2007;204:3257-3269.

6. Yoon YS, Murayama T, Gravereaux E, Tkebuchava T, Silver M, Curry C, Wecker A, Kirchmair R, Hu CS, Kearney M, Ashare A, Jackson DG, Kubo H, Isner JM, Losordo DW. VEGF-C gene therapy augments postnatal lymphangiogenesis and ameliorates secondary lymphedema. J Clin Invest. 2003;111:717-725.

7. Yoon YS, Wecker A, Heyd L, Park JS, Tkebuchava T, Kusano K, Hanley A, Scadova H, Qin G, Cha DH, Johnson KL, Aikawa R, Asahara T, Losordo DW. Clonally expanded novel multipotent stem cells from human bone marrow regenerate myocardium after myocardial infarction. J Clin Invest. 2005;115:326-338.

8. Kenyon BM, Voest EE, Chen CC, Flynn E, Folkman J, D'Amato RJ. A model of angiogenesis in the mouse cornea. Invest Ophthalmol Vis Sci. 1996;37:1625-1632.

9. Kim P, Puoris'haag M, Cote D, Lin CP, Yun SH. In vivo confocal and multiphoton microendoscopy. J Biomed Opt. 2008;13:010501.